Mechanism of leg stiffness adjustment for hopping on surfaces of different stiffnesses

CLAIRE T. FARLEY,[1] HAN H. P. HOUDIJK,[2] CISKA VAN STRIEN,[2] AND MICKY LOUIE[1]
[1]*Locomotion Laboratory, Department of Integrative Biology, University of California, Berkeley, California 94720-3140; and* [2]*Department of Human Movement Sciences, Vrije Universiteit, 1081 BT Amsterdam, The Netherlands*

Farley, Claire T., Han H. P. Houdijk, Ciska Van Strien, and Micky Louie. Mechanism of leg stiffness adjustment for hopping on surfaces of different stiffnesses. *J. Appl. Physiol.* 85(3): 1044–1055, 1998.—When humans hop in place or run forward, leg stiffness is increased to offset reductions in surface stiffness, allowing the global kinematics and mechanics to remain the same on all surfaces. The purpose of the present study was to determine the mechanism for adjusting leg stiffness. Seven subjects hopped in place on surfaces of different stiffnesses (23–35,000 kN/m) while force platform, kinematic, and electromyographic data were collected. Leg stiffness approximately doubled between the most stiff surface and the least stiff surface. Over the same range of surfaces, ankle torsional stiffness increased 1.75-fold, and the knee became more extended at the time of touchdown (2.81 vs. 2.65 rad). We used a computer simulation to examine the sensitivity of leg stiffness to the observed changes in ankle stiffness and touchdown knee angle. Our model consisted of four segments (foot, shank, thigh, head-arms-trunk) interconnected by three torsional springs (ankle, knee, hip). In the model, an increase in ankle stiffness 1.75-fold caused leg stiffness to increase 1.7-fold. A change in touchdown knee angle as observed in the subjects caused leg stiffness to increase 1.3-fold. Thus both joint stiffness and limb geometry adjustments are important in adjusting leg stiffness to allow similar hopping on different surfaces.

biomechanics; motor control; running; locomotion

LEGGED ANIMALS USE A VARIETY of gaits to move from one place to another. Despite dramatic differences in body shape and dimensions among animals, some features of their gaits are remarkably similar. For example, running, hopping, and trotting animals all move along the ground much like a bouncing ball (4, 8, 16, 22, 28). During these bouncing gaits, the actions of the body's many musculoskeletal elements, including muscles, tendons, and ligaments, are integrated together so that the overall musculoskeletal system behaves like a single spring. As a result, these gaits can be modeled by using a simple spring-mass system, consisting of a single linear "leg spring" and a point mass that is equivalent to body mass (Fig. 1) (2, 3, 6, 13–15, 18, 19, 27, 31). The stiffness of the leg spring represents the average overall stiffness of the integrated musculoskeletal system during the ground-contact phase (referred to as "leg stiffness"). In bouncing gaits, the leg spring is compressed during the first half of the ground-contact phase and lengthens during the second half of the ground-contact phase. The overall stiffness of the leg influences the mechanics and kinematics of the interaction with the ground. For example, leg stiffness affects the time of foot-ground contact and the vertical excursion of the body's center of mass (COM) during the ground-contact phase.

It is possible for the stiffness of the leg to be adjusted during bouncing gaits. When a human hops in place, a very simple bouncing gait, the stiffness of the leg is increased to increase hopping frequency or hopping height (13). Similarly, when humans run, the stiffness of the leg is adjusted to allow the use of a range of stride frequencies at a given speed (15). A stiffer leg leads to a higher stride frequency and shorter stride length at a given speed. Thus, during overground running in the natural world, it is likely that adjustments to leg stiffness allow runners to alter stride length to avoid obstacles.

Recent studies have revealed that leg stiffness is adjusted to accommodate different surfaces (18, 19). For example, when humans hop in place, leg stiffness is increased by as much as threefold to accommodate reductions in surface stiffness (18). Similarly, when humans run at a given speed, leg stiffness is adjusted to offset changes in surface stiffness (19). During both hopping in place and forward running, the adjustment to leg stiffness allows the total stiffness of the series combination of the leg and the surface to remain the same on all surfaces (18, 19). As a result, the ground-contact time and the vertical displacement of the COM during ground contact remain the same on surfaces with a 1,000-fold range of stiffnesses. If leg stiffness were not adjusted to accommodate different surfaces, both the ground-contact time and the vertical displacement of the COM would increase on lower stiffness surfaces. Thus the adjustments to leg stiffness are critical for allowing similar locomotion on surfaces of different stiffnesses.

The present study focused on the mechanisms by which leg stiffness is adjusted during bouncing gaits. To address this issue, it is important to realize that the spring-mass model represents the behavior, but not the structure, of the integrated musculoskeletal system during bouncing gaits. In reality, the length change of the leg spring that occurs during the ground-contact phase corresponds to joints flexing and extending. For example, during hopping in place, the ankle, knee, and hip flex during the first half of the ground-contact phase and extend during the second half of the ground-contact phase. In a multijointed system like the human musculoskeletal system, the overall stiffness (i.e., the leg stiffness) depends on a combination of the torsional stiffnesses of the joints and the geometry of the system. The torsional stiffness of each joint determines how much its angle changes in response to a given moment about the joint. If the ankle, knee, and hip are stiffer,

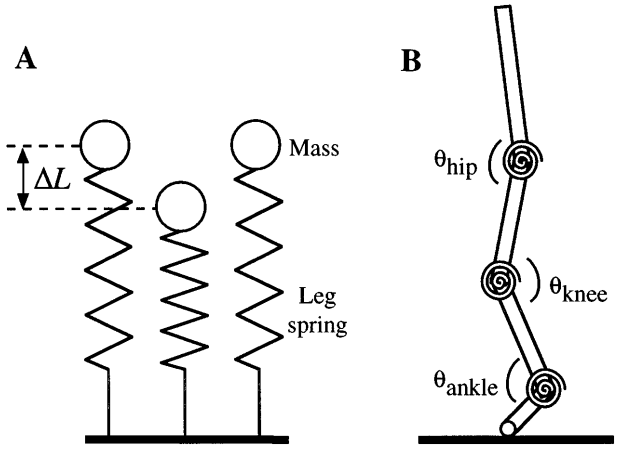

Fig. 1. *A*: spring-mass model. Single linear "leg spring" represents mechanical behavior of integrated musculoskeletal system during ground-contact phase. Mass is equivalent to body mass. Model is shown at beginning of ground-contact phase (*left*), middle of ground-contact phase (*middle*), and at end of ground-contact phase (*right*). During first half of ground-contact phase, leg spring is compressed by a distance ΔL. *B*: multijointed model used for computer simulations of hopping in place consisted of 4 segments (foot, shank, thigh, head-arms-trunk) and 3 torsional springs (ankle, knee, and hip). θ, Joint angle at instant of touchdown. See Table 1 for model parameters.

they will undergo smaller angular displacements during the ground-contact phase, resulting in less leg compression and a higher leg stiffness. Many studies have focused on joint stiffness during single-joint movements, and they have demonstrated that joint stiffness is highly adjustable. For single-joint movements involving the ankle, joint stiffness depends on many factors including muscle activation, reflexes, joint moment, and joint angle (1, 23, 30, 35, 39–42). Thus it is possible that the mechanism for adjusting leg stiffness involves adjusting the stiffness of the leg joints.

Leg stiffness during locomotion is also influenced by the geometry of the leg at the instant that the foot hits the ground ("touchdown leg geometry") (24, 32). Mathematical models predict that leg stiffness should depend on touchdown leg geometry due to changes in the alignment of the ground reaction force vector relative to the joints (24, 32). If the leg joints are more flexed when the foot hits the ground, the joint moments associated with a given ground reaction force will be greater. Thus, for a given joint stiffness, the angular displacement of the joints during the ground-contact phase also will be greater. These mathematical models have focused on how leg geometry influences leg stiffness in the absence of changes in joint stiffness. In the real musculoskeletal system, leg geometry can also influence joint stiffness because it affects muscle-tendon length and the level of muscle activation required to apply a given force to the ground (1, 23, 30, 35, 39–42). Direct experiments in humans have demonstrated the link between leg stiffness and leg geometry. When humans run with very flexed knees (32), leg stiffness is substantially lower than during normal running. Similarly, when humans bounce on a compliant board, adopting a posture with greater knee flexion leads to a lower leg stiffness (24). Finally, when humans land from a jump, the stiffness of the landing appears to depend on knee angle at landing (10). In all of these activities, it is clear that changes in leg geometry affect the alignment of the ground reaction force vector, but it is not known whether they affect joint stiffness.

The purpose of our study was to determine the mechanisms by which leg stiffness is adjusted when humans hop in place on surfaces of different stiffnesses. We began by examining the changes in joint torsional stiffness and touchdown leg geometry that occur when humans adjust their leg stiffness to accommodate surfaces of different stiffnesses. Subsequently, we explored potential mechanisms for joint stiffness adjustment by measuring the electromyographic (EMG) activity of several major leg muscles. Finally, we developed a computer simulation of human hopping in place to examine the sensitivity of leg stiffness to the changes in joint stiffness and touchdown leg geometry that we measured when subjects hopped on surfaces of different stiffnesses. In this simulation, the body was modeled with four segments (foot, shank, thigh, head-arms-trunk) interconnected by three torsional springs representing the joints (ankle, knee, hip) (Fig. 1*B*). The joint stiffnesses in the model were not affected by leg geometry. Thus we used the model to examine the effect of touchdown leg geometry on leg stiffness in the absence of any changes to joint stiffness.

METHODS

General procedures. Seven healthy subjects [3 men, 4 women, age 24.4 ± 5.0 (SD) yr, mass 59.6 ± 7.1 kg] participated in this study. Approval was obtained from the university committee for the protection of human subjects, and informed consent was given by all subjects. Subjects performed two-legged hopping on an extremely stiff surface (i.e., a force platform surface) and on sprung surfaces with four different stiffnesses. The subjects were asked to match their hopping frequency to a digital metronome that was set at 2.2 Hz. Trials were accepted if the hopping frequency was within 2% of the designated frequency. After a practice period of ~1 min at a given frequency, subjects hopped for ~30 s or until they settled into steady hopping. Subsequently, we collected kinematic, kinetic, and EMG data for a 10-s period. We chose three consecutive hops from each trial for further analysis. During all trials, the subjects kept their hands on their hips.

The subjects hopped first on the force platform, and thereafter on the sprung surfaces, progressing from the most stiff to least stiff surface. An earlier study (18) examined hopping on surfaces of different stiffnesses in a randomized order. That study focused on global aspects of hopping such as leg stiffness, peak ground reaction force, and ground-contact time. The relationship between each of these parameters and surface stiffness in the present study was virtually identical to that in the earlier study. The similarity between the findings from the earlier randomized protocol and our nonrandomized protocol suggests that the order in which the subjects hop on the surfaces of different stiffnesses does not affect hopping mechanics. In the present study, each subject performed three trials on each surface to allow collection of all the necessary data: *1*) synchronized kinematic and force platform data for calculation of joint net muscle moments and joint stiffnesses, *2*) synchronized force platform and EMG data for the lower leg muscles, and *3*) synchronized force

platform and EMG data for the upper leg muscles. Three trials were required for each condition because we had a limited number of computer analog-to-digital board inputs and EMG amplifiers. Peak ground reaction force and leg stiffness varied by <2.0 and 4.1%, respectively, among the three trials on a given surface. There were no systematic changes in either variable among the three trials ($P > 0.05$).

To test whether differences between hopping on the surfaces of different stiffnesses were statistically significant, a repeated-measures ANOVA ($P < 0.05$) was used. The statistical results (i.e., P values) reported throughout the paper are for comparisons among all five surfaces used in the study. Values are reported throughout the paper as the means ± SE.

Hopping surfaces. Subjects hopped directly on a force platform (stiffness = 35,000 kN/m; AMTI, Newton, MA) and on a sprung surface mounted on the force platform (Fig. 2). The sprung surface consisted of an aluminum honeycomb core and fiberglass sandwich panels (60 × 60 cm, Goodfellow) supported by metal compression springs (Century Spring). We adjusted the stiffness of the sprung surface by changing the number of springs supporting it. The surface was stabilized with linear bearings and metal rods to prevent lateral and horizontal movements. Despite this stabilization mechanism, the subjects reported that hopping on the sprung surface felt less stable than did hopping directly on the force platform. However, on the basis of two other studies (18, 19), we believe that the leg stiffness adjustment is a response to the change in surface stiffness rather than a response to the change in stability. The studies demonstrated that leg stiffness is adjusted to such an extent that it offsets changes in surface stiffness during hopping in place on a sprung surface and during forward running on rubber surfaces. Although the data are not reported here because of the similarity to the previous study (18), there was no change in the total stiffness of the series combination of the legs and the surface when the subjects hopped on surfaces of different stiffnesses in the present study ($P = 0.29$). In the forward-running study (19), there was no difference in stability between the rubber surfaces of different stiffnesses. This observation strongly suggests that leg stiffness adjustment is a response to a change in surface stiffness rather than a change in stability. Nonetheless, the focus of the present study was the mechanism by which leg stiffness is adjusted, and thus, we did not focus on the specific reason for the leg stiffness adjustment.

We determined the stiffness of the sprung surface from static load tests in which weights were placed on the surface and the displacement of the surface was measured. The force-displacement curve for each surface configuration was linear to within 3% over the range of forces that occurred during hopping. The stiffness of the surface was determined from the slope of the force-displacement relationship for the surface. Surface stiffnesses were 22.7, 29.6, 46.1, and 60.9 kN/m. We used the logarithmic decrement of free vibration to determine the damping ratio of the sprung surface, and we found it to be negligible (<0.005). In addition, free-vibration tests also revealed that the effective mass of the surface was 2.0 kg.

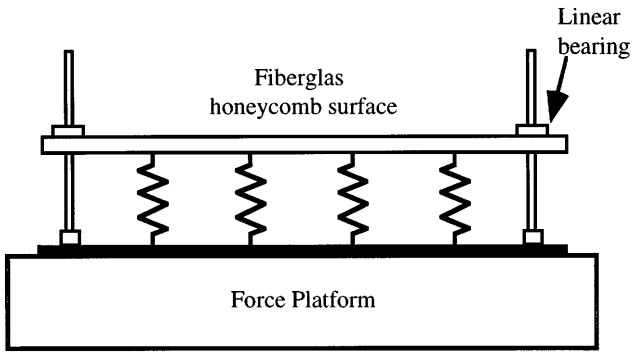

Fig. 2. Sprung surface consisted of a lightweight Fiberglas honeycomb panel supported by steel springs. Sprung surface was mounted on a force platform. Horizontal and lateral movements of panel were prevented by linear bearings.

Because the effective mass of the sprung surface was so much lower than each subject's body mass, the inertial force due to surface acceleration was negligible compared with the force exerted on the surface by the subject's feet (18). We used high-speed video analysis (200 fields/s) to determine the acceleration of the surface while subjects hopped on it. Automatic point-tracking software (Peak Performance Technologies) was used to digitize the movement of a marker fixed to the surface. Marker-position data were filtered with a fourth-order, zero-lag, low-pass Butterworth filter. The cutoff frequency was 15 Hz as determined by residual analysis (43). The maximum acceleration of the surface was 8.95 m/s^2. Thus the maximum inertial force due to surface acceleration was 17.9 N or 1.1% of the peak vertical ground reaction force on the least stiff surface. As a result, the vertical force measured with the force platform was a close approximation of the force between the subject's feet and the surface and could be used to calculate the leg stiffness.

Measurements and preliminary analyses of kinematics and kinetics data. Vertical and horizontal components of the ground reaction force were measured during each trial by using a force platform (AMTI). The force platform signals were collected at a sample frequency of 200 Hz during the first trial on each surface to match the sample frequency of the high-speed video camera (200 fields/s). In the second and third trials on each surface, the force platform signals were collected at 500 Hz to match the sample frequency for the EMG data.

For the first trial on each surface, the force platform data were used to calculate of the point of force application for the subsequent inverse dynamics analysis. The calculation of the point of force application on the sprung surface was tested by placing weights on the surface with known points of force application. These tests revealed that the calculation of the point of force application on the sprung surface was accurate to within 1.8 mm. In addition, our data showed that the position of the point of force application relative to the markers on the foot (tip of the 1st toe and 5th metatarsophalangeal joint) throughout the ground-contact phase was similar regardless of whether subjects hopped directly on the force platform or on the sprung surface.

Subjects were videotaped in lateral view at 200 fields/s (JC Labs, Mountain View, CA). Retroreflective markers were placed on the following anatomic landmarks: tip of the first toe, fifth metatarsophalangeal joint, lateral malleolus, lateral epicondyle of the femur, greater trochanter, and the acromion scapulae. Force platform and kinematic data were synchronized by using a simple circuit that simultaneously lit an LED and sent a voltage signal to the computer analog-to-digital board.

After data collection, automatic point-tracking software (Peak Performance Technologies) was used to digitize the movements of the retroreflective markers during each trial. The data for marker position were low-pass filtered by using a fourth-order zero-lag Butterworth filter with a cutoff frequency of 9 Hz (Peak Performance Technologies). The cutoff frequency was determined by using residual analysis (43). Marker-position data were used to calculate linear velocities

and accelerations of the segments as well as joint angles, segment angles, and segment angular accelerations. Each joint angle was defined by using the marker on that joint and the two adjacent markers (Fig. 1).

Calculation of leg stiffness. The technique for calculating leg stiffness during hopping on a compliant surface has been described in detail in Ferris and Farley (18). As a result, we will only describe it briefly here. The vertical movements of the COM during the ground-contact phase depended on the average leg stiffness (k_{leg}) and the surface stiffness (k_{surf}). The total vertical displacement of the subject's COM (Δy_{tot}) during the ground-contact phase was comprised of two components: the vertical displacement of the subject's COM relative to the surface (equivalent to leg spring compression, ΔL; Fig. 1*A*) and the vertical displacement of the surface (Δy_{surf})

$$\Delta y_{tot} = \Delta y_{surf} + \Delta L \quad (1)$$

The value forΔy_{tot} was calculated by twice integrating the vertical acceleration with respect to time (5, 7). The value for Δy_{surf} was calculated from the ratio of the peak vertical ground reaction force to the surface stiffness. We calculated ΔL from Δy_{tot} and Δy_{surf} by using *Eq. 1*.

The calculation of k_{leg} was made from the ratio of the ground reaction force to ΔL at the instant at the middle of the ground-contact phase when the COM reached its lowest point and the leg spring was maximally compressed (Fig. 1*A*)

$$k_{leg} = \frac{F_{peak}}{\Delta L} \quad (2)$$

The peak vertical ground reaction force (F_{peak}) occurred at the same time as the leg was maximally compressed (18). The leg stiffness, as calculated in *Eq. 2*, represents the average stiffness during the first of the ground-contact phase. Because the subjects hopped on two legs, it represents the combined stiffness of two legs.

As described in detail in Ferris and Farley (18), this calculation includes an approximation. Twice integrating the vertical ground reaction force yields the total vertical displacement of the COM of the entire system of masses that are moving on the force platform (i.e., subject and surface), rather than the vertical displacement of the subject's COM (Δy_{tot}). However, because the surface mass was small compared with a subject's body mass, the displacement of the system COM was only slightly less than the displacement of the subject's COM, leading to a maximum of a 4% overestimate of leg stiffness (18). Given that leg stiffness changed by more than twofold over the range of surface stiffnesses examined in the present study (Fig. 3*B*), we concluded that our technique for calculating the displacement of the subject's COM would provide sufficient accuracy.

Calculation of joint stiffness. The average torsional stiffnesses of the ankle, knee, and hip were determined from the ratio of the change in net muscle moment (ΔM_{joint}) to joint angular displacement ($\Delta\theta_{joint}$) in the sagittal plane between the beginning of the ground-contact phase and the instant when the joints were maximally flexed

$$k_{joint} = \frac{\Delta M_{joint}}{\Delta\theta_{joint}} \quad (3)$$

where k_{joint} is the average torsional stiffness of the joint during the first half of the ground-contact phase. The joints reached maximum flexion at approximately the same time as the COM reached its lowest point and the leg was maximally compressed. As a result, the time period for calculation of joint stiffness was nearly identical to the time period for the calculation of leg stiffness. In almost every case, the peak net muscle moment occurred at approximately the same time as the peak joint angular displacement. Joint stiffness values were calculated only in cases where the magnitude of the time difference between the occurrences of peak moment and peak angular displacement was <10% of the hop period. In these cases, the joint behaved like a torsional spring, and quantifying a joint stiffness made sense. The phase difference was always <10% except at the knee on the least stiff surface, and at the hip on the two least stiff surfaces. In the cases where the knee and hip had phase differences >10%, their angular displacements were very small (≤0.087 rad; Figs. 4 and 5). This observation, together with the results from the computer-simulation sensitivity analyses (see Fig. 9), suggests that these joints played a very small role in determining the leg stiffness under these conditions. We performed statistical analyses to determine whether joint stiffness changed in response to changes in surface stiffness in two ways: *1*) including all five surfaces and *2*) including only the three surfaces for which we had joint stiffness values for all three joints. The outcome (i.e., whether $P < 0.05$) was the same for each joint in both analyses.

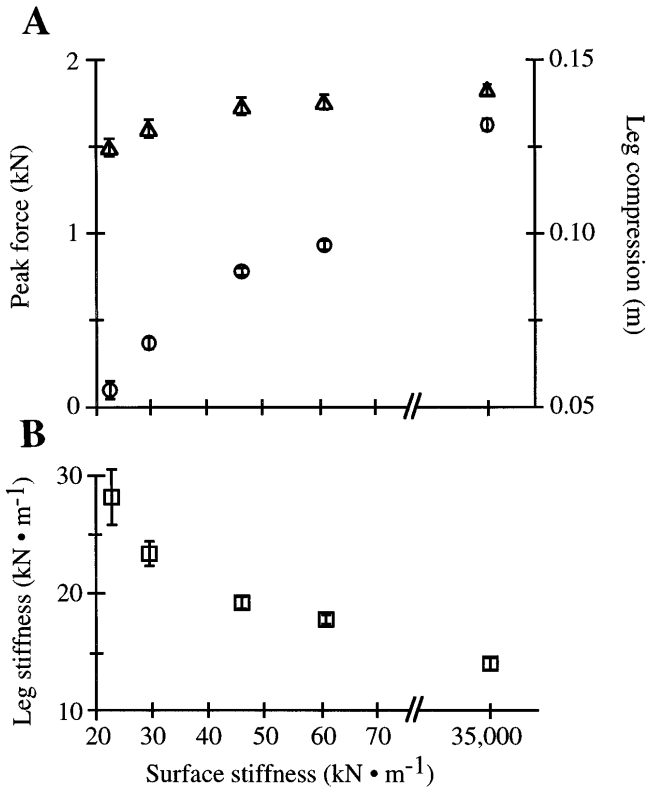

Fig. 3. *A*: peak ground reaction force (△) and leg compression (○) decreased on lower stiffness surfaces. *B*: leg stiffness (□) doubled between most stiff surface and least stiff surface. In both *A* and *B*, symbols are mean values for all subjects, and error bars are SE.

Net muscle moments were calculated by using an inverse dynamics analysis (12). This involved using force platform data and kinematic data that were collected and analyzed as described above. Anthropometric measurements in the subjects were used to calculate segment masses, segment COM locations, and segment moments of inertia (44). A rigid linked-segment model was used to calculate the net muscle moments at the ankle, knee, and hip joints (12). This involved applying Newtonian equations of angular and translational motion to each segment, starting distally and moving proximally. A net muscle moment includes the moments produced

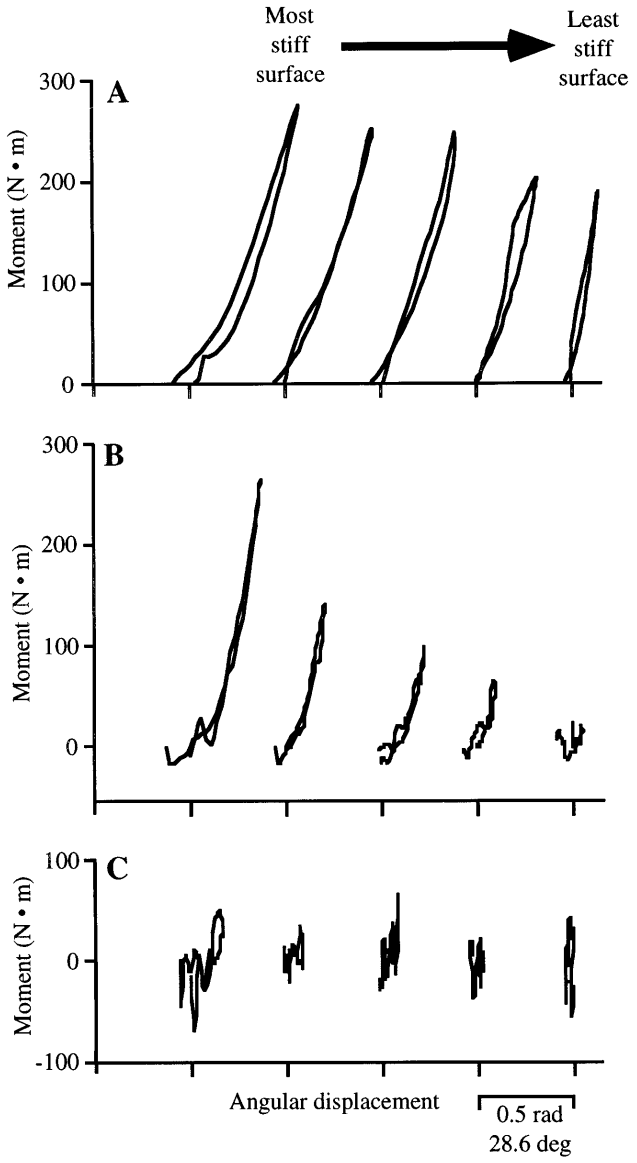

Fig. 4. Net muscle moment vs. joint angular displacement for ankle (*A*), knee (*B*), and hip (*C*) during ground-contact phase on each surface for typical subject. Positive moments represent extensor net muscle moments. Note that net muscle moment values are sum for 2 limbs. Joint angular displacement throughout ground-contact phase was calculated from difference between joint angle at touchdown and joint angle at each instant during ground-contact phase. For all joints, moving to *right* on *x*-axis indicates flexion.

by all of the muscles, tendons, ligaments, and contact forces at the joint, although the moments produced by the muscles usually dominate within the normal range of motion (21, 43). Positive net muscle moments were defined as net extensor moments. Net muscle moment and stiffness values represent the sum of the two limbs.

EMG measurements and analysis. We measured the EMG activity of six leg muscles by using surface electrodes. The muscles that we studied were the tibialis anterior, soleus, medial head of the gastrocnemius, vastus medialis, rectus femoris, and semitendinosus. In preparation for the application of the surface electrodes, the skin was shaved and prepared with fine sandpaper and alcohol. Surface EMG electrodes were placed at the approximate center of each muscle belly, with an interelectrode distance of 2 cm. The

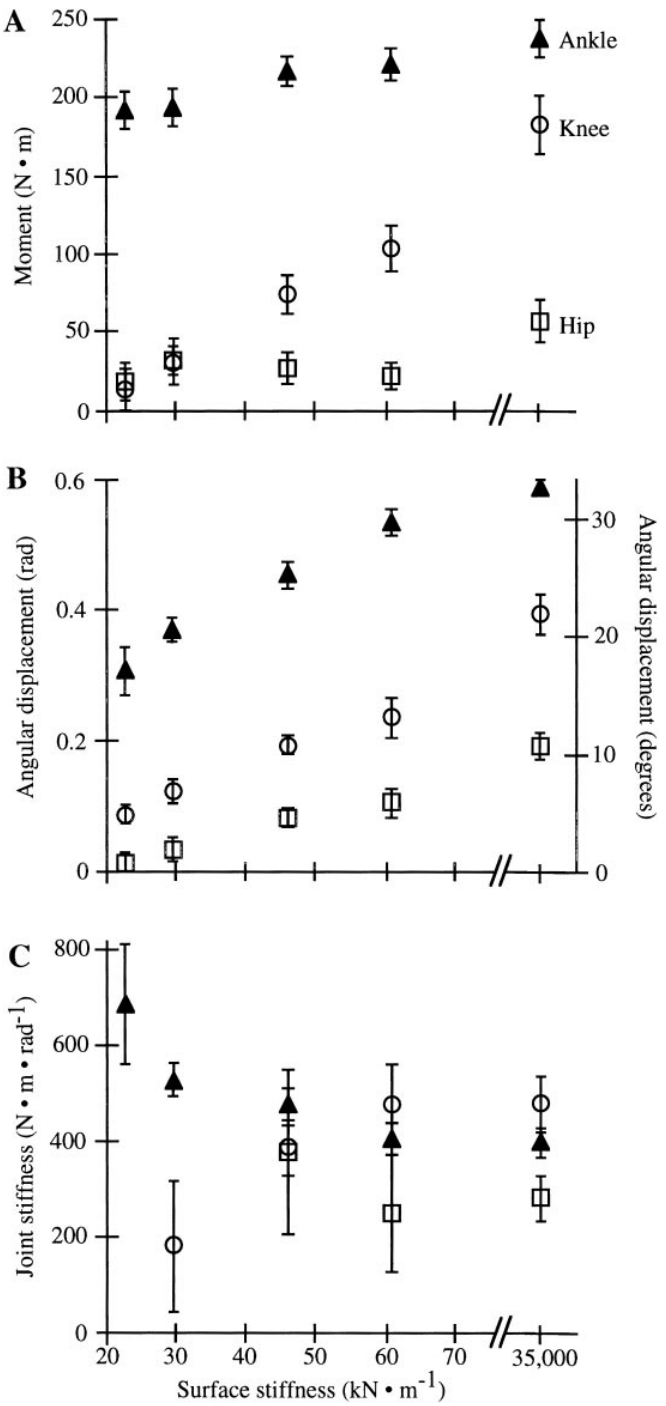

Fig. 5. *A*: net muscle moment decreased on lower stiffness surfaces for ankle (▲), knee (○), and hip (□). Net muscle moment values are for middle of ground-contact phase (i.e., when center of mass reached its lowest vertical position and joints reached maximum flexion). Note that values represent sum for 2 limbs. *B*: joint angular displacement decreased on lower stiffness surfaces for all joints. Joint angular displacement is defined as magnitude of joint flexion between beginning and middle of ground-contact phase. *C*: ankle stiffness increased on lower stiffness surfaces, whereas knee and hip stiffnesses remained the same on all surfaces. Values for symbols and error bars are defined as in Fig. 3.

electrodes remained attached between trials, and thus their location was identical for all of the trials by each subject. Elastic bandages were used to attach the wires to the subject's leg to allow unrestrained body movements and to minimize movement artifacts. The signals were band-pass filtered from 30 to 1,000 Hz and amplified 2,000 times (Grass Instruments P511, Astro-Med, Warwick, RI). The EMG signals were sampled by the computer analog-to-digital board at a frequency of 500 Hz. We performed tests in which we sampled the EMG signals at 2,000 Hz, twice as high as the high-frequency cutoff of the band-pass filter. These tests showed that the sample frequency of 500 Hz was sufficiently high to digitize the analog EMG signal without changing the timing or amplitude of the signal.

After data collection, the EMG signals were rectified and low-pass filtered with a cutoff frequency of 7 Hz, as determined by residual analysis (43), by using a fourth-order zero-lag Butterworth filter (Labview software, National Instruments). The EMG signals were normalized to the isometric maximal voluntary contraction (MVC) EMG signal for each muscle. The position of the joints during measurement of MVC closely resembled the position of the joints during hopping. The MVC EMG was measured as the experimenter opposed the maximal isometric contractions of the subjects. The area under the normalized, smoothed, rectified EMG curve (integrated EMG), representing activation level, was calculated for the contact phase and the aerial phase.

Model. We developed a computer simulation of human hopping in place for the purpose of examining the sensitivity of leg stiffness to changes in joint stiffness and geometry (Working Model Software Version 4.0, Knowledge Revolution). Our simulation used a Kutta-Merson integration method and a time step of 0.001 s. In this two-dimensional simulation, the body was modeled by using four rectangular segments (foot, shank, thigh, head-arms-trunk) and three torsional springs (ankle, knee, hip) (Fig. 1*B*). This model was designed to represent the behavior of the musculoskeletal system during hopping in place but not the mechanisms by which the neuromuscular system produces this behavior. All of the anthropomorphic, kinematic, and joint stiffness data used for building the model were based on a typical subject. Segment lengths, masses, moments of inertia, and COM locations were determined on the basis of anthropomorphic measurements from the typical subject (Table 1; see Ref. 44). Each of the leg segments represented the combined left and right segments of the human body. The head-arms-trunk segment had a mass equal to the sum of the head, two arms, and the trunk. The joint torsional springs had a linear relationship between moment and angular displacement, the slope of which was joint stiffness. The joint springs resisted flexion. Finally, the foot segment had a rounded distal end (circular arc, radius = 0.030 m). This allowed the point of contact between the model and the ground to move under the foot in a manner qualitatively similar to that observed in human subjects.

Table 1. *Model parameters*

Segment	Length, m	Mass, kg	I, kg/m²	$\theta_{segment}$ on Most Stiff Surface, rad	$\theta_{segment}$ on Least Stiff Surface, rad
HAT	0.547	45.6	1.16	0.072	0.133
Thigh	0.416	14.0	0.22	−0.139	−0.047
Shank	0.411	5.56	0.086	0.363	0.255
Foot	0.170	1.72	0.0064	−0.819	−1.107

I, moment of inertia; $\theta_{segment}$, angle of segment relative to the vertical at the instant of touchdown; HAT, head-arms-trunk. Each of the leg segments represents the combination of the left and right segments. The moment of inertia is given for rotation in the sagittal plane about the segment's center of mass. Positive values represent counterclockwise rotations.

The leg stiffness in the model was calculated from the ratio of the peak vertical ground reaction force to the peak vertical displacement of the COM of the entire model. The peak vertical ground reaction force and the peak vertical displacement of the COM occurred simultaneously (see Fig. 8). This method of calculating leg stiffness is identical to the method used to calculate leg stiffness in a human subject (*Eq. 2*).

By using the model, we examined the sensitivity of leg stiffness to changes in joint stiffness and geometry. We began by setting the initial segment positions, segment velocities, and joint stiffnesses to be the same as those measured in the typical subject at the instant that the feet hit the ground on the most stiff surface (see legends for Table 1 and Fig. 8 for values). When the simulation was run, the model interacted with an infinitely stiff surface (i.e., the ground), and we measured the leg stiffness during the ground-contact phase. The model was surprisingly stable and could complete multiple hops in which the movements of the COM and joint angular displacements were similar from one hop to the next. All of the data presented in Figs. 8 and 9 were from the first ground-contact phase of the simulation.

We performed several sensitivity analyses to determine the separate influences of joint stiffness and leg geometry on leg stiffness. Our starting point was always the segment configuration and joint stiffnesses that corresponded to hopping on the most stiff surface, as described above. By using this starting point, we began by examining the sensitivity of leg stiffness to changes in the stiffness of each of the joints. Subsequently, we examined the sensitivity of leg stiffness to the change in limb geometry observed in our subjects between the most stiff surface and the least stiff surface (Table 1). From these sensitivity analyses, we were able to determine the separate effects of the changes in joint stiffness and limb geometry that we measured when the subjects hopped on different surfaces.

RESULTS

When subjects hopped on surfaces of different stiffnesses, leg stiffness increased as surface stiffness decreased (Fig. 3*B*). Leg stiffness more than doubled from 13.9 kN/m on the most stiff surface to 28.1 kN/m on the least stiff surface ($P < 0.0001$). Leg stiffness is equal to the ratio of the peak ground reaction force to leg compression (*Eq. 2*). Peak ground reaction force decreased by 17% between the most stiff surface and the least stiff surface ($P = 0.017$; Fig. 3*A*). Leg compression decreased by ~60% from 0.131 m on the most stiff surface to 0.055 m on the least stiff surface ($P < 0.0001$; Fig. 3*A*).

To determine the mechanism for leg stiffness adjustment, we began by examining the stiffness of the joints. Figure 4 shows typical examples of net muscle moment vs. angular displacement curves for the ankle, knee, and hip joints during the ground-contact phase. Angular displacement was defined as the change in joint angle relative to the joint angle at the instant that the feet hit the ground. From Fig. 4*A*, it can be seen that, as the feet hit the ground, the net muscle moment at the ankle began to rise. During this phase, the ankle flexed,

as demonstrated by the increasing angular displacement. The ankle net muscle moment and angular displacement reached their maximum values simultaneously. Then, during the second half of the contact phase, the ankle moment decreased as the ankle extended and the COM moved upward. The ankle moment reached a value of zero at approximately the time when the feet left the ground. The slope of the ankle moment vs. angular displacement relationship increased on lower stiffness surfaces, indicating that ankle stiffness increased. The shape of the relationship between net muscle moment and angular displacement was similar at the knee as at the ankle (Fig. 4*B*). As surface stiffness decreased, the net muscle moment and angular displacement at the knee decreased, and there was no noticeable change in the slope of the relationship. The net muscle moment and the angular displacement were smaller at the hip than at either the ankle or knee (Fig. 4*C*).

As surface stiffness decreased from the most stiff to the least stiff surface, the ankle stiffness increased 1.75-fold (Fig. 5*C*). We calculated the joint stiffness only when the phase shift between peak moment and peak angular displacement was <10% of that during the hopping period. The phase shift was always <10% at the ankle (mean for all trials = 0.37 ± 0.85%). The ankle stiffness increased significantly ($P = 0.023$) between the most stiff surface and the least stiff surface (396.0 vs. 687.0 N·m/rad). This increase in ankle stiffness led to a 50% decrease in ankle angular displacement ($P = 0.003$; Fig. 5*B*) despite a relatively slight decrease (19%) in peak net muscle moment ($P = 0.022$; Fig. 5*A*).

The knee and hip stiffnesses did not change with surface stiffness ($P = 0.18$ and 0.53, respectively; Fig. 5*C*). We did not calculate stiffness values when the phase between the peak moment and the peak angular displacement was >10%. The phase was 12.7% at the knee during hopping on the least stiff surface and was 10.5 and 12.4% for the hip during hopping on the two least stiff surfaces (k_{surf} = 29.6 and 22.7 kN/m, respectively). In all of these cases, the angular displacement and net muscle moment at the joint were very small. At both joints, the net muscle moment and the angular displacement decreased as surface stiffness decreased ($P < 0.001$ for all; Fig. 5, *A* and *B*).

Subjects landed with straighter knees on less stiff surfaces. The knee angle at touchdown increased between the most stiff surface and the least stiff surface (2.65 ± 0.01 vs. 2.81 ± 0.01 rad; $P < 0.001$) (Fig. 6*A*). This change in knee geometry led to a reduction in the mean moment arm of the ground reaction force about the knee on the least stiff surface compared with the most stiff surface (0.001 vs. 0.054 m; $P < 0.001$) (Fig. 6*B*). The ankle and hip angles at touchdown did not change with surface stiffness ($P = 0.41$, $P = 0.21$, respectively).

We measured the EMG signals from several limb muscles to determine whether joint stiffness was adjusted by changing muscle activation. In nearly all of the muscles examined, we found that the area under

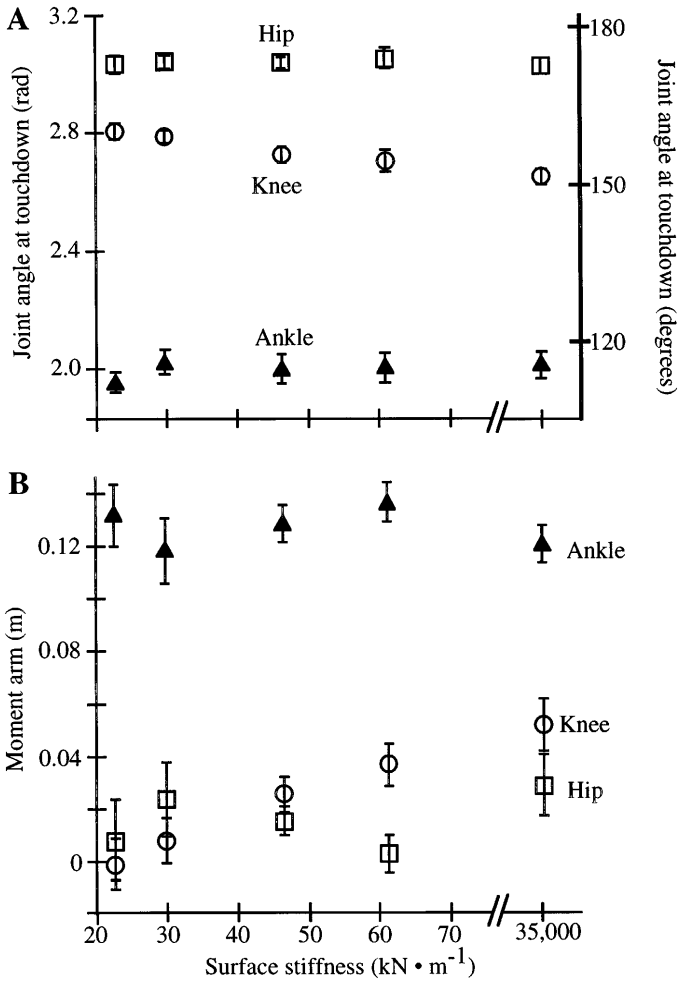

Fig. 6. *A*: joint angle at touchdown increased as surface stiffness decreased for knee (○) but remained similar on all surfaces for ankle (▲) and hip (□). See Fig. 1 for joint angle definitions. *B*: mean moment arm of ground reaction force during ground-contact phase decreased on lower stiffness surfaces for knee but remained the same on all surfaces for ankle and hip. Values for symbols and error bars are defined as in Fig. 3.

the ground-contact-phase EMG decreased as surface stiffness decreased (Fig. 7, Table 2). Significant reductions in EMG during the ground-contact phase were observed in the soleus (−26%), gastrocnemius (−22%), vastus medialis (−70%), rectus femoris (−61%), and semitendinosus (−25%) ($P < 0.001$ for all; Table 2). The exception was the tibialis anterior, for which the area under the ground-contact-phase EMG was independent of surface stiffness ($P = 0.998$). The timing of EMG relative to the beginning of the ground-contact phase did not change with surface stiffness (Fig. 7). Thus the observed increase in ankle stiffness as surface stiffness decreased was not due to increased activation or changes in activation timing of the muscles acting about the ankle.

Our computer model allowed us to examine the sensitivity of leg stiffness to the observed changes in joint stiffness and leg geometry found in the experiments when the subjects hopped on surfaces of different stiffnesses. We began by comparing the relationship

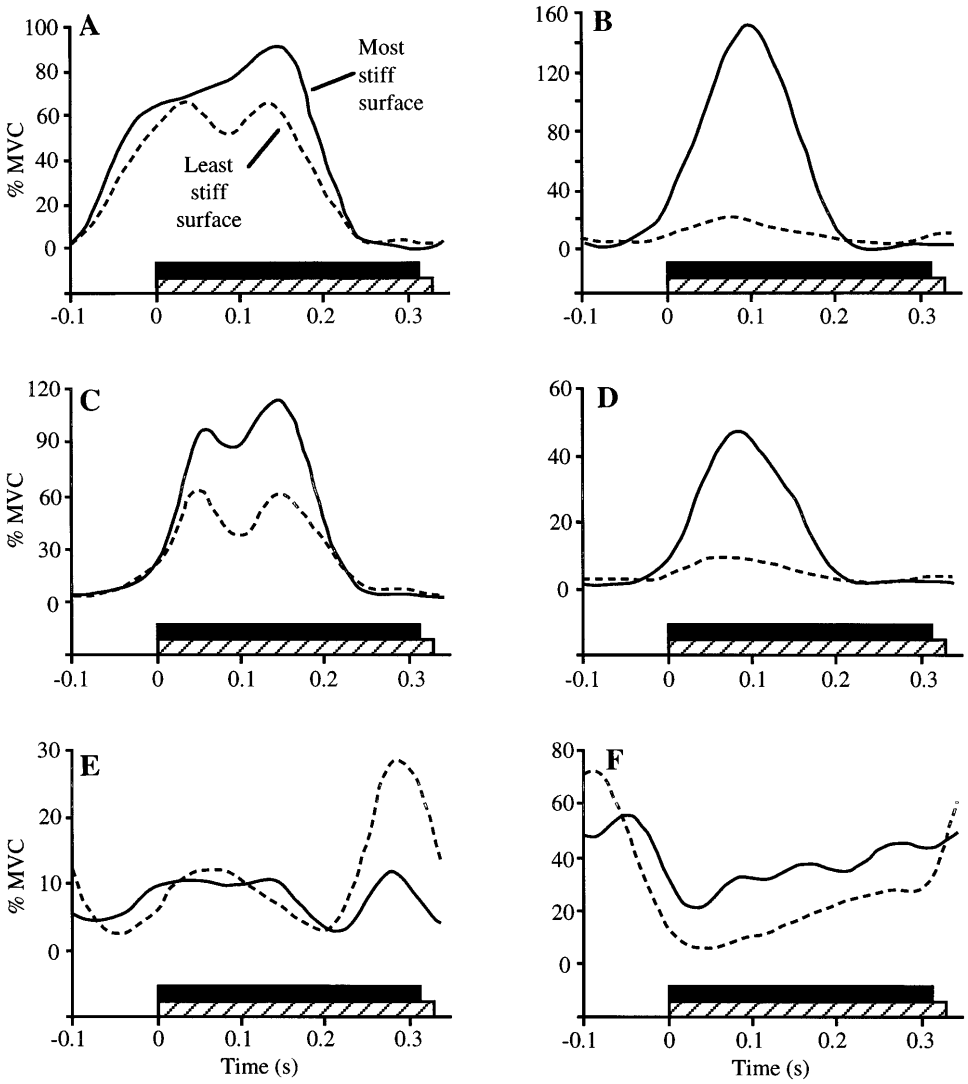

Fig. 7. Electromyographic data from typical subject. *A–F*: gastrocnemius, vastus medialis, soleus, rectus femoris, tibialis anterior, and semitendinosus muscles, respectively. Solid lines, data for hopping on most stiff surface; dashed lines, data for hopping on least stiff surface; solid bars, ground-contact time on most stiff surface; hatched bars, ground-contact time on least stiff surface. Ground-contact phase started at *time 0* on both surfaces. MVC, maximal voluntary contraction.

between the vertical ground reaction force and the vertical displacement of the COM for a typical subject and the model (Fig. 8). For the typical subject, the force-displacement relationship is shown for hopping on the most stiff surface and the least stiff surface. For the model, the first force-displacement relationship was generated with the joint stiffnesses and the leg geometry set to the values measured in a typical

Table 2. *Integrated EMG values during the ground-contact phase and the aerial phase*

k_{surf}, kN/m	TA, %·s	Sol, %·s	Gast, %·s	VM, %·s	RF, %·s	ST, %·s
			Ground-contact phase			
35,000	3.76 ± 1.33	14.75 ± 5.82	16.69 ± 6.53	13.11 ± 6.70	4.04 ± 2.06	5.62 ± 4.41
60.9	3.47 ± 1.42	13.27 ± 4.92	14.37 ± 6.63	6.67 ± 3.61	2.42 ± 2.12	3.90 ± 3.01
46.1	3.33 ± 1.06	12.13 ± 5.12	13.64 ± 5.81	5.87 ± 2.64	2.51 ± 1.81	4.53 ± 4.21
29.6	3.28 ± 1.16	10.57 ± 4.17	12.88 ± 5.98	4.68 ± 1.92	1.82 ± 1.38	4.45 ± 3.61
22.7	4.95 ± 1.56	10.95 ± 4.66	12.94 ± 6.52	3.97 ± 1.91	1.58 ± 1.11	4.18 ± 3.69
			Aerial phase			
35,000	1.92 ± 1.15	0.85 ± 0.59	3.01 ± 1.08	0.73 ± 0.50	0.30 ± 0.34	2.39 ± 1.75
60.9	1.92 ± 1.44	1.11 ± 0.53	3.59 ± 0.99	0.79 ± 0.48	0.32 ± 0.18	2.17 ± 2.01
46.1	1.68 ± 0.82	0.94 ± 0.42	2.68 ± 0.87	0.78 ± 0.43	0.32 ± 0.18	2.26 ± 2.11
29.6	1.59 ± 0.80	1.09 ± 0.56	2.96 ± 1.51	0.77 ± 0.36	0.31 ± 0.21	2.50 ± 2.75
22.7	0.86 ± 0.46	1.20 ± 0.65	3.13 ± 1.82	0.75 ± 0.38	0.28 ± 0.14	1.79 ± 1.94

Values are means ± SE; $n = 7$ subjects. EMG, electromyographic signal; k_{surf}, surface stiffness; TA, tibialis anterior; Sol, soleus; Gast, medial gastrocnemius; VM, vastus medialis; RF, rectus femoris; ST, semitendinosus. Integrated EMG was calculated from the integral of the EMG, expressed as % maximal voluntary contraction, with respect to time. Thus the units are %·s.

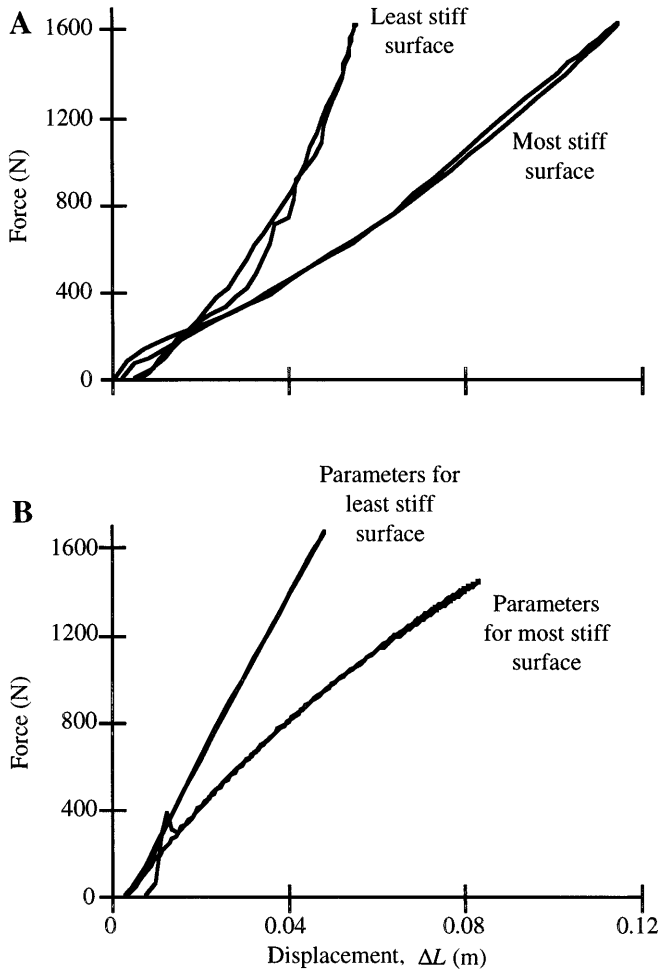

Fig. 8. *A*: force vs. downward displacement of center of mass (i.e., ΔL) for typical subject hopping on most stiff surface and least stiff surface. *B*: force vs. ΔL for model. *Bottom* curve, data for model with joint stiffness values and touchdown segment configuration observed in typical subject hopping on most stiff surface ("parameters for most stiff surface"; Table 1). In this case, joint stiffnesses were 361 N·m/rad for ankle, 363 N·m/rad for knee, and 415 N·m/rad for hip. Subsequently, ankle stiffness was increased by 1.75-fold, and touchdown segment configuration was changed to match that of typical subject hopping on least stiff surface (*top* curve, "parameters for least stiff surface," Table 1).

subject hopping on the most stiff surface ("most stiff surface parameters"). Subsequently, ankle stiffness and the configuration of the body segments were changed to the values measured in a typical subject hopping on the least stiff surface ("least stiff surface parameters"). In both the subject and the model, the average slope of the force-displacement relationship approximately doubled between the two conditions. In the typical subject, leg stiffness increased from 14.3 to 29.4 kN/m between the most stiff surface and the least stiff surface. In the model, leg stiffness increased from 17.1 to 34.9 kN/m. The observation of a similar change in leg stiffness for the subject and the model suggests that leg stiffness depends on joint stiffness and leg geometry similarly in the model and in an actual human hopper. Thus the model can provide insight into the sensitivity of leg stiffness to the stiffness of the joints and leg geometry.

It is also interesting to note that there were differences in the shape of the force-displacement curves between the model and subject. In the model, the slope of the force-displacement relationship was greatest immediately after touchdown. In the subject, this slope was lowest immediately after touchdown. During the middle of the contact phase, the slopes of the force-displacement curves were similar for both. Mainly due to the difference immediately after touchdown, the model underwent a smaller vertical displacement of its COM and had a higher average leg stiffness for the contact phase than did the subject.

We found that the leg stiffness of the model was most sensitive to changes in ankle stiffness (Fig. 9). For example, when ankle stiffness was increased 1.75-fold, as observed in our subjects between the most stiff and least stiff surfaces, leg stiffness increased 1.7-fold. In contrast, changing the knee or hip stiffness in the model had a much smaller effect on leg stiffness (Fig. 9). Doubling knee stiffness increased leg stiffness by 8%, and doubling hip stiffness increased leg stiffness by 3%.

We also used the computer model to determine the sensitivity of leg stiffness to the change in knee angle at touchdown that we measured in our subjects when they hopped on surfaces of different stiffnesses. We began by setting the joint stiffnesses and segment configuration to match the values measured for a typical subject hopping on the most stiff surface. Subsequently, we kept the joint stiffnesses the same but changed the configuration of the body segments to the values measured for the typical subject at the instant of touchdown

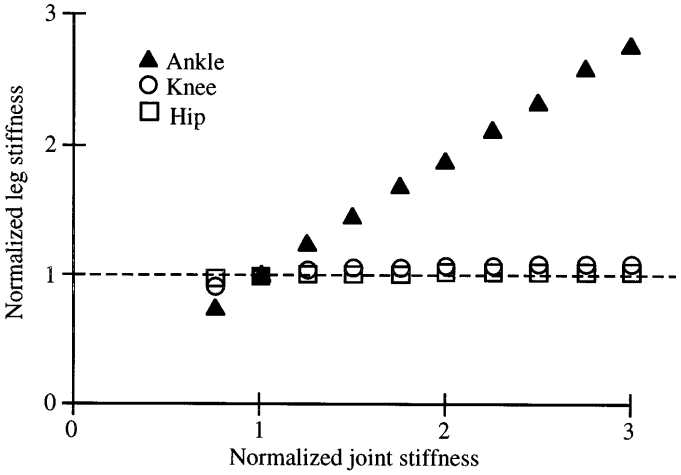

Fig. 9. Model predictions for sensitivity of leg stiffness to changes in stiffness of each joint. "Normalized joint stiffness" is ratio of joint stiffness in that simulation to joint stiffness used during hopping on most stiff surface. "Normalized leg stiffness" is ratio of leg stiffness in that simulation to leg stiffness used during hopping on most stiff surface. Data for each joint were obtained by keeping stiffness of other 2 joints and leg geometry the same as on most stiff surface and then systematically changing stiffness of joint of interest. ▲, Data from simulations in which ankle stiffness was systematically changed while other parameters were kept the same; ○ and □, data from simulations in which knee and hip stiffnesses, respectively, were systematically changed. Joint stiffness values on most stiff surface were 361 N·m/rad for ankle, 363 N·m/rad for knee, and 415 N·m/rad for hip.

on the least stiff surface (Table 1). This change in touchdown geometry caused a 1.3-fold increase in leg stiffness (17.1 vs. 22.2 kN/m). Thus we concluded that the change in geometry played an important role in the adjustment of leg stiffness, although the adjustment to ankle stiffness had a larger effect on leg stiffness.

DISCUSSION

Leg stiffness is adjusted to offset differences in surface stiffness during hopping in place or forward running (18, 19). As a result, the total stiffness of the series combination of the legs and the surface remains the same regardless of surface stiffness (18, 19). Consequently, humans are able to keep the global mechanics and kinematics of hopping in place or forward running the same on different surfaces. For example, the ground-contact time, stride frequency, and vertical displacement of the COM during the contact phase are similar on surfaces of different stiffnesses. The purpose of our study was to determine the mechanisms by which leg stiffness is adjusted when humans hop in place on surfaces of different stiffnesses.

Our findings demonstrate that adjustments to ankle stiffness are most important in adjusting leg stiffness. Over the range of surfaces that we examined, leg stiffness increased by twofold to accommodate reductions in surface stiffness. Ankle stiffness increased 1.75-fold over the same range in surface stiffnesses, whereas the knee and hip stiffnesses do not change. Leg geometry also changed; the knee was more extended at touchdown on lower stiffness surfaces. An analysis using our computer model revealed that leg stiffness is very sensitive to changes in ankle stiffness. A 1.75-fold increase in ankle stiffness led to a 1.7-fold increase in leg stiffness in the model. Changing touchdown knee angle as observed in our subjects caused a 1.3-fold increase in leg stiffness. Finally, simultaneously changing ankle stiffness and touchdown knee angle produced a doubling of leg stiffness in the model, just as observed in hopping subjects. Thus leg stiffness is adjusted for different surfaces by a combination of changes in ankle stiffness and knee angle.

Despite the simplicity of the computer model, it simulates human hopping in place reasonably accurately. When leg geometry and joint stiffnesses are set to the values for a typical subject hopping on the most stiff surface, the leg stiffness of the model is 19% higher than is the leg stiffness of the subject. Examination of the force-displacement relationships (Fig. 8) reveals that the model is stiffer shortly after touchdown than is a typical subject. This may be due to a difference in the moment-angular displacement relationship for the joints of subjects compared with the model. In the subjects, both the ankle and knee are less stiff shortly after touchdown than later in the contact phase (Fig. 4). As a result, the slope of the force-displacement relationship for the leg follows the same pattern; it is low early in the contact phase and increases later in the contact phase. In contrast, the model has constant-stiffness joints and thus has a higher leg stiffness at the beginning of the contact phase than does an actual human hopper. Despite these differences, the model's leg stiffness doubles when ankle stiffness and touchdown knee angle are simultaneously changed, as observed in the subjects between the most stiff surface and the least stiff surface. In the human subjects, leg stiffness also doubles between the most stiff surface and the least stiff surface. The similar change in leg stiffness in the human subjects and the model suggests that the model can give insight into the separate effects on leg stiffness of changing ankle stiffness and touchdown knee angle.

On the basis of sensitivity analyses, it is clear that leg stiffness is very sensitive to changes in ankle stiffness but is much less sensitive to changes in knee or hip stiffness (Fig. 9). Despite the complexity of the leg, its stiffness is nearly directly proportional to the stiffness of a single joint, the ankle. Moreover, the knee and hip can have a range of stiffness values without substantially affecting leg stiffness. Our findings show that knee and hip stiffness remain the same when humans adjust their leg stiffness in response to a change in surface stiffness. In addition, knee and hip stiffnesses are more variable than is ankle stiffness. We could not quantify the knee or hip stiffness when the subjects hopped on very low stiffness surfaces because the net muscle moment and angular displacement were not in phase with each other. As a result, our analysis may not adequately describe the behavior of the knee and hip in these situations. However, it seems very unlikely that their behavior is involved in the adjustment of leg stiffness. This conclusion is based on the observation that the behavior of the knee and hip had only a slight effect on leg stiffness in our model (Fig. 9).

The selective sensitivity of leg stiffness to ankle stiffness is not due to differences in stiffness values for the three joints. In a system with multiple springs, the least stiff spring undergoes the largest displacement in response to a force and has the most influence on the overall stiffness. However, the ankle is not the least stiff joint during hopping in place (Fig. 5). Alternative explanations are that leg stiffness is particularly sensitive to ankle stiffness because of the geometry of the leg or because of the distal position of the ankle within the leg. Because of the leg's geometry, the moment arm of the ground reaction force is largest about the ankle (Fig. 6). Therefore, a given ground reaction force will be associated with a larger net muscle moment and angular displacement at the ankle than at the knee or hip (Fig. 5). In addition, rotation of the foot segment, a parameter directly affected by ankle stiffness, will lead to a larger vertical excursion of the COM than will rotation of any other segment. This is because the foot segment is closer to horizontal than any other segment and because of its distal position within the leg.

Previous observations suggest that the important role of ankle stiffness in the adjustment of leg stiffness may extend to other movements and other animals (9, 11). A comparison of leg stiffness between a single landing and hopping in place in humans demonstrated that the differences in leg stiffness ("whole body stiffness") are paralleled by differences in ankle stiffness (11). Similarly, in a small bipedal bird, changes in leg

stiffness are paralleled by changes in ankle stiffness during running and during landing from a jump (9). Finally, previous studies of landings and drop jumps in humans have shown that the pattern of moment and angular displacement at the joints changes depending on surface stiffness and whether the subject intended to land stiffly or compliantly (10, 33, 34, 37, 38). Although joint stiffness was not reported, the data suggest that joint stiffness varied depending on the task.

It is not obvious how ankle stiffness is adjusted for hopping on surfaces of different stiffnesses. A variety of techniques have been used to examine the modulation of joint stiffness during single-joint movements (1, 17, 20, 23, 35, 39, 41, 42). Although many factors affect joint stiffness, it is clear that joint stiffness strongly depends on the level of activation of the muscles acting about the joint. Thus the ankle could be made stiffer by increasing the activation of the gastrocnemius or soleus, or by increasing the coactivation of the tibialis anterior, an ankle flexor muscle (11, 35, 40). However, our findings show that there is no increase in EMG activity in the gastrocnemius, soleus, or tibialis anterior over the range of surface stiffnesses where ankle stiffness increases 1.75-fold (Fig. 7). Indeed, our data show a decrease in activation in the gastrocnemius and soleus. This observation shows that ankle stiffness during hopping is not adjusted by changing the level of muscle activation. Alternatively, it is conceivable that ankle stiffness is adjusted by changing limb geometry because the stiffness of the muscle-tendon units crossing the ankle varies depending on their length (23, 41, 42). The touchdown ankle angle did not change on different surfaces, but the touchdown knee angle increased on lower stiffness surfaces (Fig. 6*A*). The gastrocnemius muscle-tendon unit crosses both the ankle and knee, and thus gastrocnemius stiffness and ankle stiffness could be affected by the touchdown knee angle. However, given the small change in touchdown knee angle, it seems unlikely that it could have produced a 1.75-fold change in ankle stiffness. This conclusion is based on the gastrocnemius force-length relationship and the dependence of gastrocnemius length on knee angle in humans (25, 29). A final alternative explanation is that the stiffness of the muscles crossing the ankle could be adjusted by changing the firing frequency of the active motor units (26) or by recruiting different motor units (36). These possibilities should be explored in future studies.

As demonstrated by this study, our approach to understanding the link between the mechanics of locomotion and the mechanical properties of the musculoskeletal elements begins at the global level and sequentially moves toward lower levels of organization. The musculoskeletal system comprises multiple segments interconnected by joints. Each joint has numerous muscles, tendons, and ligaments acting about it. Given the complexity of the control of the stiffness of a single muscle or joint, it would be extremely difficult to use a forward dynamics approach that begins at the level of individual muscles and attempts to explain the control of locomotion. Instead, we have used an inverse dynamics approach that began by characterizing the rules governing the relationship between the global mechanics and kinematics of locomotion and leg stiffness. The present study reveals that leg stiffness is extremely sensitive to the stiffness of the ankle. This finding makes it obvious that the next step is to examine the neuromuscular mechanisms for adjusting ankle stiffness during locomotion. Thus, because of our progression from the global level to lower levels of organization, we can now formulate focused hypotheses about how individual elements of the musculoskeletal system contribute toward determining the kinematics and mechanics of locomotion at the global level. At this point in the progression, an approach that combines behavioral modeling (e.g., the models used in the present study) with more realistic neuromuscular models may reveal important principles about the control of bouncing gaits.

This research was supported by National Institute of Arthritis and Musculoskeletal and Skin Diseases Grant R29 AR-44008 (C. T. Farley).

Address for reprint requests: C. T. Farley, Locomotion Laboratory, Dept. of Integrative Biology, 3060 Valley Life Sciences Bldg., Univ. of California, Berkeley, CA 94720-3140 (E-mail: cfarley@socrates.berkeley.edu).

Received 9 September 1997; accepted in final form 1 May 1998.

REFERENCES

1. **Agarwal, G. C., and G. L. Gottlieb.** Oscillation of the human ankle joint in response to applied sinusoidal torque on the foot. *J. Physiol. (Lond.)* 268: 151–176, 1977.
2. **Alexander, R. M.** *Elastic Mechanisms in Animal Movement*. Cambridge, UK: Cambridge Univ. Press, 1988.
3. **Blickhan, R.** The spring-mass model for running and hopping. *J. Biomech*. 22: 1217–1227, 1989.
4. **Blickhan, R., and R. J. Full.** Locomotion energetics of ghost crab. II. Mechanics of the center of mass during walking and running. *J. Exp. Biol*. 130: 155–174, 1987.
5. **Blickhan, R., and R. J. Full.** Mechanical work in terrestrial locomotion. In: *Biomechanics: Structures and Systems*, edited by A. A. Biewener. New York: Oxford Univ. Press, 1993, p. 75–96.
6. **Blickhan, R., and R. J. Full.** Similarity in multilegged locomotion: bouncing like a monopode. *J. Comp. Physiol. [A]* 173: 509–517, 1993.
7. **Cavagna, G. A.** Force platforms as ergometers. *J. Appl. Physiol*. 39: 174–179, 1975.
8. **Cavagna, G. A., N. C. Heglund, and C. R. Taylor.** Mechanical work in terrestrial locomotion: two basic mechanisms for minimizing energy expenditure. *Am. J. Physiol*. 233 (*Regulatory Integrative Comp. Physiol*. 2): R243–R261, 1977.
9. **Clark, B.** *Mechanics and Control of the Limb of Bobwhite Quail Running and Landing on Substrates of Unpredictable Mechanical Stiffness* (PhD thesis). Chicago, IL: Univ. of Chicago, 1988.
10. **Devita, P., and W. A. Skelly.** Effect of landing stiffness on joint kinetics and energetics in the lower extremity. *Med. Sci. Sports Exerc*. 24: 108–115, 1992.
11. **Dyhre-Poulsen, P., E. B. Simonsen, and M. Voigt.** Dynamic control of muscle stiffness and H reflex modulation during hopping and jumping in man. *J. Physiol. (Lond.)* 437: 287–304, 1991.
12. **Elftman, H.** Forces and energy changes in the leg during walking. *Am. J. Physiol*. 125: 339–356, 1939.
13. **Farley, C. T., R. Blickhan, J. Saito, and C. R. Taylor.** Hopping frequency in humans: a test of how springs set stride frequency in bouncing gaits. *J. Appl. Physiol*. 71: 2127–2132, 1991.
14. **Farley, C. T., J. Glasheen, and T. A. McMahon.** Running springs: speed and animal size. *J. Exp. Biol*. 185: 71–86, 1993.

15. **Farley, C. T., and O. Gonzalez.** Leg stiffness and stride frequency in human running. *J. Biomech*. 29: 181–186, 1996.
16. **Farley, C. T., and T. C. Ko.** Two basic mechanisms in lizard locomotion. *J. Exp. Biol*. 200: 2177–2188, 1997.
17. **Feldman, A. G.** Superposition of motor programs. I. Rhythmic forearm movements in man. *Neuroscience* 5: 81–90, 1980.
18. **Ferris, D. P., and C. T. Farley.** Interaction of leg stiffness and surface stiffness during human hopping. *J. Appl. Physiol*. 82: 15–22, 1997.
19. **Ferris, D. P., M. Louie, and C. T. Farley.** Running in the real world: adjustments in leg stiffness for different locomotion surfaces. *Proc. Roy. Soc. B*. 265: 989–994, 1998.
20. **Fitzpatrick, R. C., J. L. Taylor, and D. I. McClosky.** Ankle stiffness of standing humans in response to imperceptible perturbation: reflex and task-dependent components. *J. Physiol. (Lond.)* 454: 533–547, 1992.
21. **Fowler, E. G., R. J. Gregor, J. A. Hodgson, and R. R. Roy.** Relationship between ankle muscle and joint kinetics during the stance phase of locomotion in the cat. *J. Biomech*. 26: 465–483, 1993.
22. **Full, R. J., and M. S. Tu.** Mechanics of six-legged runners. *J. Exp. Biol*. 148: 129–146, 1990.
23. **Gottlieb, G. L., and G. C. Agarwal.** Dependence of human ankle compliance on joint angle. *J. Biomech*. 11: 177–181, 1978.
24. **Greene, P. R., and T. A. McMahon.** Reflex stiffness of man's anti-gravity muscles during kneebends while carrying extra weights. *J. Biomech*. 12: 881–891, 1979.
25. **Grieve, D. W., S. Pheasant, and P. R. Cavanagh.** Prediction of gastrocnemius length from knee and ankle posture. In: *Biomechanics VI-A*, edited by E. Asmussen and K. Jorgensen. Baltimore, MD: University Park, 1978, p. 405–412.
26. **Grillner, S.** The role of muscle stiffness in meeting the changing postural and locomotor requirements for force development by the ankle extensors. *Acta Physiol. Scand*. 86: 92–108, 1972.
27. **He, J. P., R. Kram, and T. A. McMahon.** Mechanics of running under simulated low gravity. *J. Appl. Physiol*. 71: 863–870, 1991.
28. **Heglund, N. C., G. A. Cavagna, and C. R. Taylor.** Energetics and mechanics of terrestrial locomotion. III. Energy changes of the centre of mass as a function of speed and body size in birds and mammals. *J. Exp. Biol*. 97: 41–56, 1982.
29. **Herzog, W., L. J. Read, and H. E. D. J. Ter Keurs.** Experimental determination of force-length relations of intact human gastrocnemius muscles. *Clin. Biochem*. 6: 230–238, 1991.
30. **Hunter, I. W., and R. E. Kearney.** Dynamics of human ankle stiffness: variation with mean ankle torque. *J. Biomech*. 15: 747–752, 1982.
31. **McMahon, T. A., and G. C. Cheng.** The mechanics of running: how does stiffness couple with speed? *J. Biomech*. 23, *Suppl*. 1: 65–78, 1990.
32. **McMahon, T. A., G. Valiant, and E. C. Frederick.** Groucho running. *J. Appl. Physiol*. 62: 2326–2337, 1987.
33. **McNitt-Gray, J. L., T. Yokoi, and C. Millward.** Landing strategies used by gymnasts on different surfaces. *J. Appl. Biomech*. 10: 237–252, 1994.
34. **McNitt-Gray, J. L., T. Yokoi, and C. Millward.** Landing strategy adjustments made by female gymnasts in response to drop height and mat composition. *J. Appl. Biomech*. 9: 173–190, 1993.
35. **Nielsen, J., T. Sinkjaer, E. Toft, and Y. Kagamihara.** Segmental reflexes and ankle joint stiffness during co-contraction of antagonistic ankle muscles in man. *Exp. Brain Res*. 102: 350–358, 1994.
36. **Petit, J., G. M. Filippi, F. Emonet-Denand, C. C. Hunt, and Y. Laporte.** Changes in muscle stiffness produced by motor units of different types in peroneus longus muscle of cat. *J. Neurophysiol*. 63: 190–197, 1990.
37. **Sanders, R. H., and J. B. Allen.** Changes in net joint torques during accommodation to change in surface compliance in a drop jumping task. *Hum. Mov. Sci*. 12: 299–326, 1993.
38. **Sanders, R. H., and B. D. Wilson.** Modification of movement patterns to accommodate to a change in surface compliance in a drop jumping task. *Hum. Mov. Sci*. 11: 593–614, 1992.
39. **Sinkjaer, T., E. Toft, S. Andreassen, and B. C. Hornemann.** Muscle stiffness in human ankle dorsiflexors: intrinsic and reflex components. *J. Neurophysiol*. 60: 1110–1121, 1988.
40. **Weiss, P. L., I. W. Hunter, and R. E. Kearney.** Human ankle joint stiffness over the full range of muscle activation levels. *J. Biomech*. 21: 539–544, 1988.
41. **Weiss, P. L., R. E. Kearney, and I. W. Hunter.** Position dependence of ankle joint dynamics–I. Passive mechanics. *J. Biomech*. 19: 727–735, 1986.
42. **Weiss, P. L., R. E. Kearney, and I. W. Hunter.** Position dependence of ankle joint dynamics–II. Active mechanics. *J. Biomech*. 19: 737–751, 1986.
43. **Winter, D. A.** *Biomechanics and Motor Control of Human Movement*. New York: Wiley, 1990.
44. **Zatsiorsky, V., and V. Seluyanov.** The mass and inertial characteristics of the main segments of the human body. In: *Biomechanics VIII-B*, edited by H. A. K. Matsui. Champaign, IL: Human Kinetics, 1983, p. 1152–1159.